First-principle study of the structural, electronic, and optical properties of SiC nanowires*

Wei-Hu Zhang(张威虎)[1], Fu-Chun Zhang(张富春)[2,†], Wei-Bin Zhang(张伟斌)[3], Shao-Lin Zhang(张绍林)[3], and Woochul Yang[3,‡]

[1] *Communication and Information Engineering College, Xi'an University of Science and Technology, Xi'an* 710068, *China*
[2] *College of Physics and Electronic Information, Yan'an University, Yan'an* 716000, *China*
[3] *Department of Physics, Dongguk University, Seoul* 100715, *Korea*

(Received 16 October 2016; revised manuscript received 13 January 2017; published online 6 April 2017)

We preform first-principle calculations for the geometric, electronic structures and optical properties of SiC nanowires (NWs). The dielectric functions dominated by electronic interband transitions are investigated in terms of the calculated optical response functions. The calculated results reveal that the SiC NW is an indirect band-gap semiconductor material except at a minimum SiC NW ($n = 12$) diameter, showing that the NW ($n = 12$) is metallic. Charge density indicates that the Si–C bond of SiC NW has mixed ionic and covalent characteristics: the covalent character is stronger than the ionic character, and shows strong s–p hybrid orbit characteristics. Moreover, the band gap increases as the SiC NW diameter increases. This shows a significant quantum size and surface effect. The optical properties indicate that the obvious dielectric absorption peaks shift towards the high energy, and that there is a blue shift phenomenon in the ultraviolet region. These results show that SiC NW is a promising optoelectronic material for the potential applications in ultraviolet photoelectron devices.

Keywords: SiC, first-principle calculation, nanowires, electronic structure

PACS: 71.15.Mb, 73.90.+f, 78.67.–n **DOI:** 10.1088/1674-1056/26/5/057103

1. Introduction

Silicon carbide (SiC) is one of the better known IV–IV wide band gap semiconductor materials due to its unique properties. It is interesting and well known for its high temperature, large power, high frequency, resistance to radiation, short luminescent wavelength, and usage in optical electronic integrated devices.[1–7] When compared with similar semiconductor materials, SiC also has a high chemical stability, high electron saturation velocity, large critical breakdown of electric field, low thermal expansion coefficient, high heat conductivity, super high radio resistance, and several other advantages.[8,9] Presently, SiC NWs are receiving a great deal of attention due to the rapid development of poly-type materials, such as SiC nanotubes, nanoclusters, and nanorods.[10–12] This is because SiC is a low-dimensional nano-material that has a higher length-to-diameter ratio and higher surface area. It shows different properties in its bulk form in the fields of photology, electrology, thermology, and magnetics. Another reason for the considerable interest in SiC NWs is their unique structural, mechanical, electronic, magnetic, and optical characteristics. Many research groups have made significant efforts to synthesize the SiC NWs. Shi *et al.*[13] adopted a method in which a laser is used to ablate a SiC target material at a high temperature of 900 °. Their results showed that the NWs were evenly distributed with a uniform configuration and superior photoelectric properties. Cheng *et al.*[5] prepared SiC nano-materials by using the gas–liquid–solid method. Apparent quantum size and surface effects were revealed. Zhou *et al.*[14] used an electro-spinning technique to prepare SiC nanosticks by using rare-earth metals as a catalyst. The results indicated that the threshold electric field was 8 V/m. Huang *et al.*[15] reported a graphene/SiC-based self-powered UV photodetector that exhibits a photocurrent responsivity of 7.4 mA/W. Yu *et al.*[16] prepared SiC NWs by mechanical mixing, the results indicated that the average thermal conductivity of suspensions with SiC NWs is greatly improved. In addition, β-SiC NWs are the potential photoelectric materials and show great diverse applications for the next generation of devices in the fields of optical, energy area, biomedical engineering, nanoelectronics, and microelectronics. Liu *et al.*[17] synthesized β-SiC NWs via a facile chemical vapor deposition (CVD) method at 1300 °C, the product showed a narrow diameter of about 50 nm, was highly curved and had good flexibility with the catalyst. Dai *et al.*[18] prepared β-SiC NWs via a simple CVD method with using Si/SiO_2 powders at 1460 °C. Liu *et al.*[19] synthesized SiC NWs by using low pressure chemical vapor infiltration (LPCVI) in a porous graphite substrate with-

*Project supported by the National Natural Science Foundation of China (Grant No. 61664008), the Special Research Funds for Discipline Construction of High Level University Project, China (Grant No. 2015SXTS02), the Basic Science Research Program through the National Research Foundation of Korea (NRF) funded by the Ministry of Education (Grant Nos. 2015R1D1A1A01058991 and 2016R1A6A1A03012877).

†Corresponding author. E-mail: zhangfuchun72@163.com
‡Corresponding author. E-mail: wyang@dongguk.edu

© 2017 Chinese Physical Society and IOP Publishing Ltd

out using a catalyst. The results indicated that SiC nanowires were β-SiC that grew in clusters and were curved.

To date, most of SiC material studies have focused on experimental preparation without in-depth discussion on the internal mechanism regarding structures and properties. As a result, there are many unanswered questions requiring more in-depth study of the structure and properties of SiC nanomaterials. In this paper, we directly address these issues in order to provide a theoretical basis for experimental preparation of high-quality low-dimensional SiC nanomaterials.

2. Theoretical models and calculation methods

2.1. Theoretical models

The NW model is developed from a SiC wurtzite crystal structure. In order to build different-diameter SiC NWs, the SiC wurtzite crystal atoms are cut along six external NW layer surfaces as shown in Fig. 1. The SiC NW diameters increase from 0.31 to 2.15 nm, and there are 192, 108, 48, 26 and 12 atoms in each NW configuration as shown in Fig. 2. To minimize the interaction between surfaces due to the finite supercells, the SiC NWs are placed in a square supercell with a vacuum thickness of 1 nm.

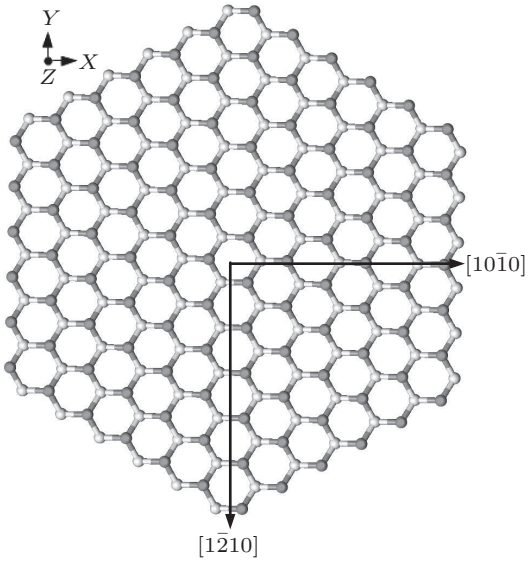


Fig. 1. Top view of SiC NW (dark and white spheres represent C and Si atoms, respectively).

2.2. Calculation methods

First-principle calculations based on the density functional theory (DFT)[20] with a plane wave pseudo-potential[21] basis are performed by using the Vienna *ab initio* simulation package (VASP).[20,22] The detailed parameter settings are shown as follows. Pseudo potential is described by using the pseudo potential of projector augmented waves (PAW).[23] The wave function is optimized by the conjugate gradient method. Exchange–correlation potential is considered as the Generalized Gradient Approximation (GGA)[24] in the form of Perdew–Burke–Ernzerhof.[25] The chosen valence-electron configurations for atoms are Si-$3s^2 3p^2$ and C-$2s^2 2p^2$, respectively. The cutoff energy of the plane wave is set to be 360 eV. The maximum root-mean-square convergent tolerance is less than 1×10^{-6} eV. The maximal displacement convergence is 1×10^{-4} nm, and internal stress is less than 0.1 GPa. The Brillouin zone integration is approximated by using the special K-points sampling scheme of Monkhorst Pack and $1\times1\times32$ k-point grids are used.

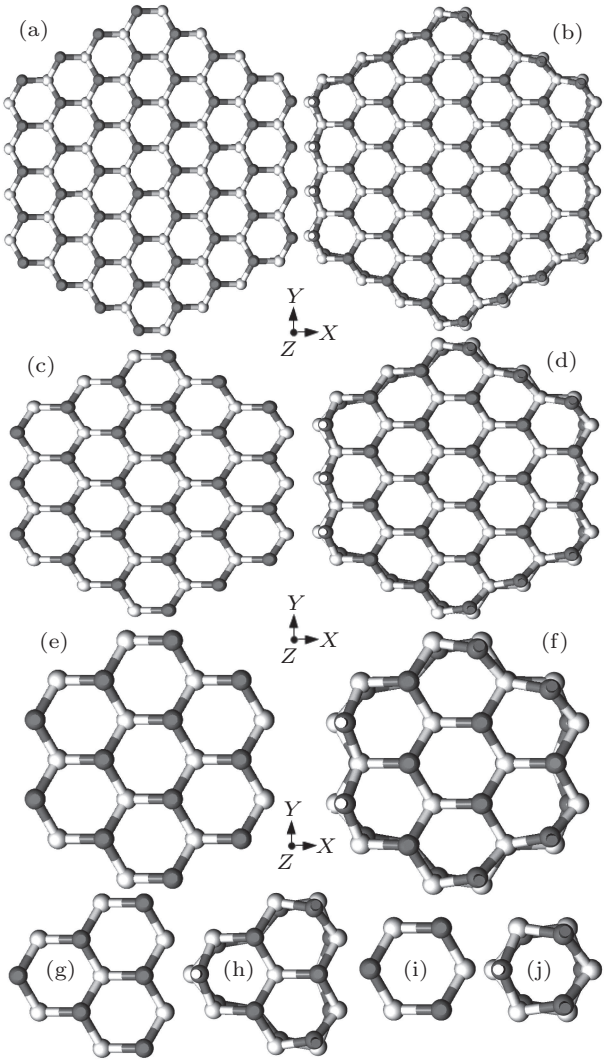


Fig. 2. Structural models of SiC NWs, showing ((a), (c), (e), (g), (i)) unoptimized structures, ((b), (d), (f), (h), (j)) optimized structures, where the dark and white spheres represent C and Si atoms, respectively.

In the linear response range, the optical response function is generally described by a dielectric function $\varepsilon(\omega) = \varepsilon_1(\omega) + \mathrm{i}\varepsilon_2(\omega)$, with

$$\varepsilon_1 = n^2 - k^2, \tag{1}$$

$$\varepsilon_2 = 2nk, \tag{2}$$

where n and k are defined as reflection and extinction coefficients, respectively.

According to the definitions of direct transition and joint density of states between the conductions and valence bands,

we can deduce that an imaginary part and a real part of the dielectric function are as follows:[26]

$$\varepsilon_2 = \frac{C_1}{\omega^2}\sum_{\mathrm{V,C}}\int_{\mathrm{BZ}} \mathrm{d}^3\boldsymbol{K}\frac{2}{(2\pi)}|\boldsymbol{e}\cdot\boldsymbol{M}_{\mathrm{CV}}(\boldsymbol{K})|^2 \times \delta[\boldsymbol{E}_{\mathrm{C}}(\boldsymbol{K}) - E_{\mathrm{V}}(\boldsymbol{K}) - \hbar\omega], \quad (3)$$

$$\varepsilon_1 = 1 + C_2\sum_{\mathrm{V,C}}\int_{\mathrm{BZ}} \mathrm{d}^3\boldsymbol{K}\frac{2}{(2\pi)}\frac{|\boldsymbol{e}\cdot\boldsymbol{M}_{\mathrm{CV}}(\boldsymbol{K})|^2}{[\boldsymbol{E}_{\mathrm{C}}(\boldsymbol{K}) - E_{\mathrm{V}}(\boldsymbol{K})]} \times \frac{\hbar^3}{[\boldsymbol{E}_{\mathrm{C}}(\boldsymbol{K}) - E_{\mathrm{V}}(\boldsymbol{K})]^2 - \hbar^2\omega^2}, \quad (4)$$

where BZ refers to the first Brillouin zone, $\boldsymbol{K}$ is the reciprocal lattice vector, $\hbar$ is the Planck constant, $|\boldsymbol{e}\cdot\boldsymbol{M}_{\mathrm{CV}}(\boldsymbol{K})|^2$ is the dynamic transition matrix element, ω refers to angular frequency, C_1 and C_2 both refer to constants, while $E_{\mathrm{C}}(K)$ and $E_{\mathrm{V}}(K)$ are the energy levels on conduction band and valence band, respectively. The above relations are used as the theoretical basis for analyzing photonic crystal band structures and optical properties.

3. Results and discussion

3.1. Geometric structures and stability analysis

Initially, we optimize the atomic structure of periodic one-dimensional (1D) SiC NWs. As shown in Figs. 2(b)–2(j), the Si and C atoms gradually move towards the internal and outer layer NWs, respectively. Here the Si atoms move 0.15–0.25 Å and the C atoms only shift 0.02–0.05 Å. As the SiC NW diameter increases, large atomic relaxations are only observed in the outer layers of Si and C atoms. This shows a great quantum size effect and surface effect.

Figure 3 displays the variations of the binding energy and band gap with dimension of SiC NWs. We find that the band gap is zero, and NW appears metallic (corresponding to the minimum SiC NW). However, as the NW diameter increases further, the band gap increases and appears to have semiconductor properties. Our calculated band gap (corresponding to the maximum SiC NW) is about 1.83 eV, which is consistent with the experimental value of bulk material.[27,28] The calculated results clearly show that SiC NWs possess a lower binding energy, and the binding energy decreases according to a linear rate law with NW diameter increases. Furthermore, the value of the band gap depends on the diameter and NWs become more stable with diameter increases.

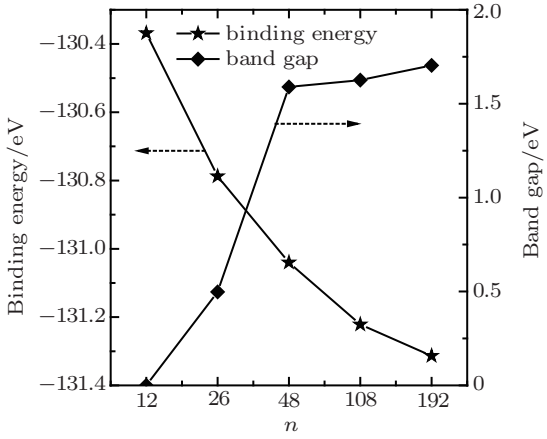


Fig. 3. The binding energy and band gap of SiC NWs.

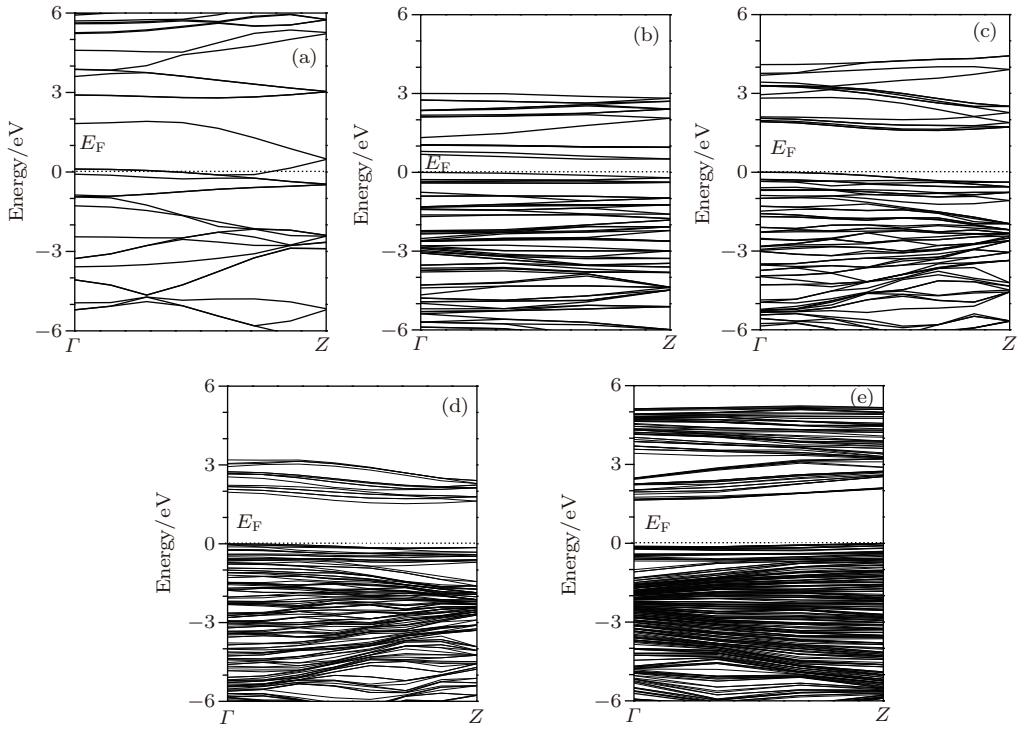


Fig. 4. Energy band structures of SiC NWs for different values of the atomic number of (a) $n = 12$, (b) $n = 26$, (c) $n = 48$, (d) $n = 108$, (e) $n = 192$.

As shown in Fig. 4, the band structures are obtained along the direction Γ (0, 0, 0)→ Z (0, 0, 0.5) of the high symmetry point of the SiC NW Brillouin zone. Many unique features are present in the different band structure dimensions with different SiC NWs sizes. From Fig. 4(a) it is clearly seen that the NW is metallic and that the energy levels at the top of valence band and at the bottom of the conduction band pass through a Fermi level. However, all the remaining SiC NWs exhibit the features of an indirect band-gap semiconductor with NW diameter increasing. At the same time, the top of the valence band lies at the high Brillouin zone symmetry point Γ (0, 0, 0), and the bottom of the conduction band lies at the high Brillouin zone symmetry point Z (0,0,0.5). This is similar to the energy band structure of bulk SiC.[29] In particular, when the number of atoms in the NW is equal to $n = 192$ as shown in Fig. 4(e), we can see that there is an apparent change in the energy band structure, while the top of the valence band remains at point Z (0, 0, 0.5) in the Brillouin zone and the bottom of the conduction band is still at Point Γ (0, 0, 0) in the Brillouin zone. The valence band shows large dispersivity but the conduction band then exhibits localization features. In addition, the band gap gradually increases with the increase of SiC NW diameter, and the bottom of the conduction band moves along the [001] direction from point Γ to point Z with diameter decreasing. The above results show that the SiC NW experiences a blue shift phenomenon, which is consistent with those obtained from experiment and the theory of ZnO, GaN, and SiC materials.[30–34] The trend is more predictable at larger diameters; therefore, an abnormal blue shift phenomenon is significant for designing blue and ultraviolet light semiconductor devices.

To further investigate the SiC NW properties, we calculate the projected electronic density of states (PDOS). From Fig. 5 it follows that the SiC NW valence bands are mainly composed of the upper valence bands (−9.0 eV–0.0 eV) and the lower valence bands (−15.0 eV––10.0 eV). From the PDOS we can clearly see that the upper valence bands are mainly composed of C-2p and Si-3p states together and present dramatic s–p hybridization properties, which is consistent with existing theoretical and experimental results. At the same time, the width of the upper valence band is increased from 8.0 eV ($n = 24$) to 9.0 eV ($n = 192$), and the total DOS moves towards low energy with the increase of the SiC NW diameter. However, the DOS peaks tend to be less intense with the increase of the NW diameter. This is mainly because of quantum confinement and surface effects, leading to reduced localization. For large-diameter SiC NWs, the DOS tends to be closer to that of bulk SiC. Moreover, the lower valence bands are mainly composed of 2s and 2p states and have s–p orbital hybridization distribution properties. As for the conduction bands of SiC NWs, we can see that it is mainly composed of 2p and 2s states of C and Si atoms from PDOS. The total DOS moves towards high energy, resulting in an increase of the band gap. This is consistent with the analyses of the above band structures, and it is observed that an apparent surface state appears on the bottom of the conduction band and the top of the valence band, respectively. The positions and intensities of these peaks are of significance for the nature of SiC NWs, which can have a direct influence on their properties.

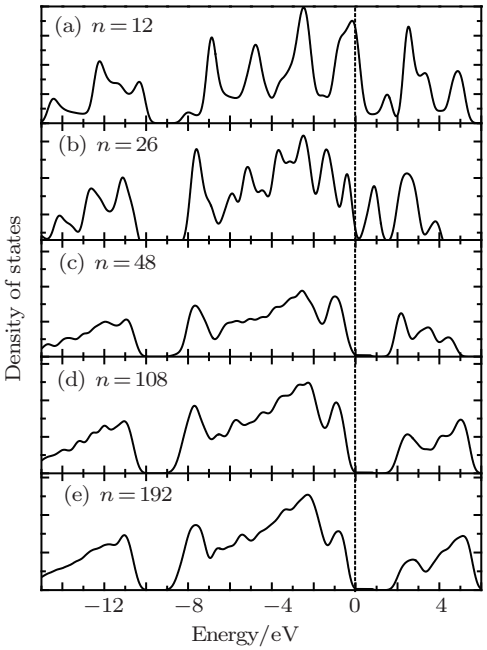


Fig. 5. Total DOSs of SiC NWs.

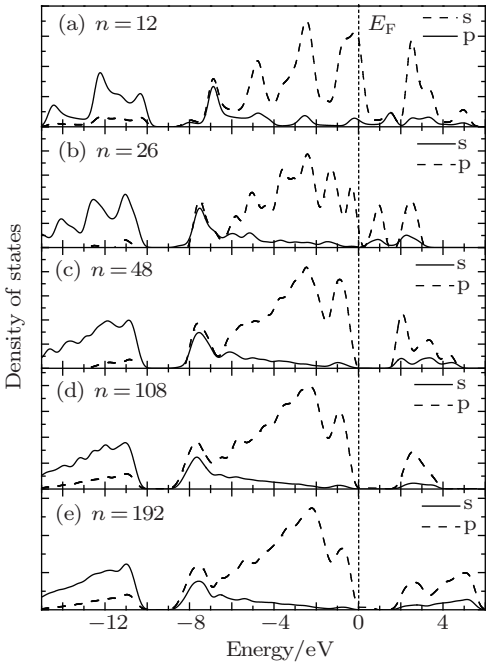


Fig. 6. PDOSs of SiC NWs.

In Fig. 7, we illustrate the total densities of SiC NWs ($n = 108$, $n = 192$) showing the electron cloud distributions. We observe that a typical mixed valence of Si and C atoms and

the SiC NWs appear to have a strong covalent character rather than an ionic character. The electrons mainly converge at the surrounding C atoms, but are centered on the axial line of the SiC NW and distributed along the direction of the diameter. Covalent bonds at different layers of the SiC NW increase, and the electrons mainly converge around the C atoms while both C and Si atoms apparently form s–p hybridized distribution properties. In addition, on the external atoms, an irregular electron distribution appears. Electrons at the external electronic layer are forced to move towards the center of the NW, and electrons on Si atoms are forced to move towards the external layer, which exhibits a dramatic surface effect.

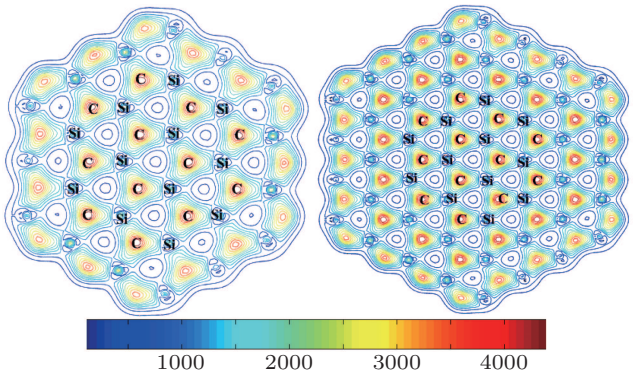


Fig. 7. (color online) Plots of electron density of SiC NWs along the [0001] direction for the cases of $n = 108$ and 192.

The imaginary and real parts of the dielectric constant of SiC NWs with different diameters are shown in Figs. 8(a) and 8(b). The imaginary and real parts can be divided into a low energy region (0–3.0 eV) and a high energy region (3.0–8.0 eV). From the above band structures and DOS analysis, the dielectric peaks in the low energy region are derived from a transition of the maximum occupied states (top of the valence band) to the minimum unoccupied states (bottom of the conduction band). The values of the first dielectric peaks in the low-energy region decrease with increasing diameter. This is mainly caused by the fact that the bottom of the conduction band of SiC NWs becomes far from the top of the valence band with increasing diameter, which gives rise to the decrease of the transition probability of electrons. In the higher energy region, the intensity of dielectric peak dramatically decreases and only at ~ 4.0 eV does a weaker dielectric transition peak appear. According to the above band structures and DOSs, we can deduce that these dielectric peaks are mainly derived from a transition of Si 3p state to C 2s state. In addition, with increasing diameter, the strongest dielectric peaks in the low energy region move towards higher energy. This is consistent with the trend of the band gap mentioned above. The results indicate that the dielectric constant has an obvious blue shift and the absorption spectrum band edge wavelength corresponds to the ultraviolet zone. Therefore, SiC NWs may also be superior ultraviolet photoelectron materials.

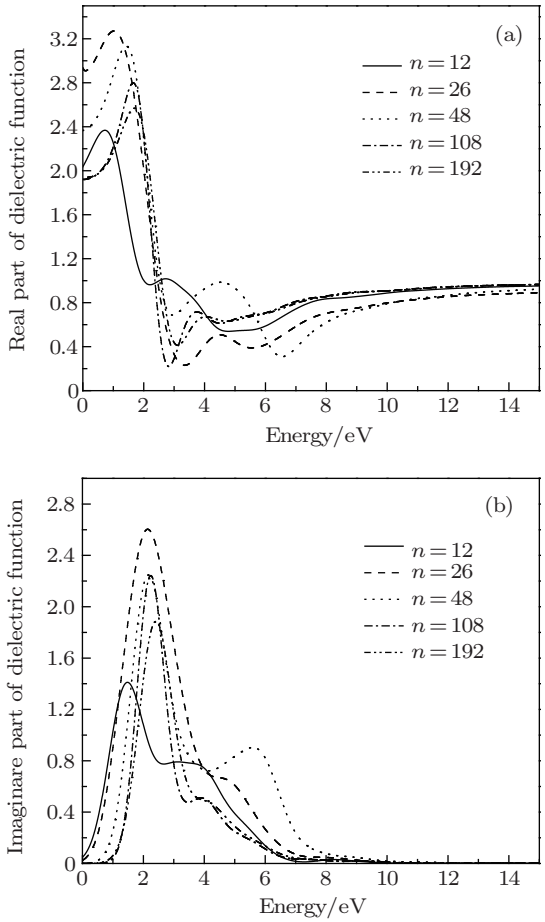


Fig. 8. Dielectric functions of SiC NWs, showing the variations of (a) real part ε_1 and (b) imaginary part ε_2 with energy.

4. Conclusions

In summary, the first-principles calculations of SiC NWs and the geometric and band structures are carried out, and the DOS, charge density, and optical properties are analyzed. Our results show that the external Si and C atoms experience a dramatic relaxation, causing an increase of the NW specific surface area. This increase is larger than that of bulk SiC due to the quantum size effect and surface effect. The SiC NWs are an indirect band gap semiconductor and the top of the valence band and the bottom of the conduction band exhibit large dispersivity and localization features, respectively, and the chemical bonds of SiC NWs are formed by the overlap of s–p hybridized orbitals. The optical properties reveal that the dielectric peaks in the low energy region move towards higher energy and indicate that the absorption edge has an obvious blue shift with the increase of SiC NW size. The dielectric peak is closer to the ultraviolet range. The calculated results indicate that the SiC NW is a superior type of ultraviolet photoelectron material.

References

[1] Wong E W, Sheehan P E and Lieber C M 1997 *Science* **277** 1971
[2] Prasai D, John W, Weixelbaum L, Krüger O, Wagner G, Sperfeld P, Nowy S, Friedrich D, Winter S and Weiss T 2013 *J. Mater. Res.* **28** 33

[3] Anderson T J, Hobart K D, Greenlee J D, Shahin D I, Koehler A D, Tadjer M J, Imhoff E A, Myers-Ward R L, Christou A and Kub F J 2015 *Appl. Phys. Express* **8** 041301
[4] Gao R X, Gao S Y, Fan G H, Liu J, Wang Q, Zhao H F and Qu S L 2014 *Acta Phys. Sin.* **63** 067801 (in Chinese)
[5] Cheng G M, Chang T H, Qin Q Q, Huang H C and Zhu Y 2014 *Nano Lett.* **14** 754
[6] Liu H T, Huang Z H, Fang M H, LiuY G and Wu X W 2015 *J. Cryst. Growth* **419** 20
[7] Hua Y, Wan H, Chen X Y, Wu P and Bai S X 2016 *Acta Phys. Sin.* **65** 168102 (in Chinese)
[8] Niu J J, Wang J N and Xu N S 2008 *Solid State Sci.* **10** 618
[9] She Q, Jiang M F, Qian N and Pan Y 2014 *Acta Phys. Sin.* **63** 185204 (in Chinese)
[10] Aldalbahi A, Li E, Rivera M, Velazquez R, Altalhi T, Peng X Y and Feng P X 2016 *Sci. Rep.* **6** 23457
[11] Chiew Y L and Cheong K Y 2012 *J. Mater. Sci.* **47** 5477
[12] Yu W, Wang M Z, Xie H Q, Hu Y H and Chen L F 2016 *Appl. Therm. Eng.* **94** 350
[13] Shi W, Zheng Y, Peng H, Wang N, Lee C S and Lee S T 2000 *J. Am. Ceram. Soc.* **83** 3228
[14] Zhou J Y, Chen Z Y, Xu X B, Zhou M, Ma Z W, Zhao J G, Li R S and Xie E Q 2010 *J. Amer. Ceram. Soc.* **93** 488
[15] Huang J, Guo L W, Lu W, Zhang Y H, Shi Z, Jia Y P, Li Z L, Yang J W, Chen H X, Mei Z X, and Chen X L 2016 *Chin. Phys. B* **25** 067205
[16] Yu W, Wang M Z, Xie H Q, Hu Y H, Chen L F 2016 *Appl. Therm. Eng.* **94** 350
[17] Liu S L, Liu H T, Huang Z H, Fang M H, Liu Y G and Wu X W 2016 *RSC Adv.* **6** 24267
[18] Dai J X, Sha J J, Zhang Z F, Wang Y C and Krenkel W 2015 *Ceram. Int.* **41** 9637
[19] Liu Y S, Men J, Feng W, Cheng L F and Zhang L T 2014 *Ceram. Int.* **40** 11889
[20] Kresse G and Furthmüller J 1996 *Phys. Rev. B* **54** 11169
[21] Payne M C, Teter M P, Arias T A, Allan D C and Joannopoulos J D 1992 *Rev. Mod. Phys.* **64** 1045
[22] Kresse G and Hafener J 1994 *Phys. Rev. B* **49** 14251
[23] Perdew J P, Burke K and Ernzerhof M 1996 *Phys. Rev. Lett.* **77** 3865
[24] Kresse G and Joubert D 1999 *Phys. Rev. B* **59** 1758
[25] Perdew J P and Wang Y 1992 *Phys. Rev. B* **45** 13244
[26] Read A J and Needs R J 1991 *Phys. Rev. B* **44** 13071
[27] Lu B, Liu J X, Zhu H W and Jiao X H 2007 *Mater. Sci. Forum.* **561** 1413
[28] Pan H and Feng Y P 2008 *ACS Nano* **2** 2410
[29] Xu Y N and Ching W Y 1993 *Phys. Rev. B* **48** 4335
[30] Wang Z L 2004 *Materials Today* **7** 26
[31] Zou X C, Wu M S, Liu G, Ouyang C Y and Xu B 2013 *Acta Phys. Sin.* **62** 107101 (in Chinese)
[32] Huang M H, Mao S, Feick H, Yan H Q, Wu Y Y, Kind H, Weber E, Russo R and Yang P 2001 *Science* **292** 1897
[33] Unalan H E, Zhang Y, Hiralal P, Dalal S, Chu D, Eda G, Teo K B K, Chhowalla M and Milne W I 2009 *Appl. Phys. Lett.* **94** 163501
[34] Gao S P and Zhu T 2012 *Acta Phys. Sin.* **61** 137103 (in Chinese)